Tropical Plant Pathology (2023) 48:174–181
https://doi.org/10.1007/s40858-023-00555-y

ORIGINAL ARTICLE

Histological changes at the seedling growth (Z12) and stem elongation (Z31) stages after *Tilletia controversa* infection

Mekuria Wolde[1] · Zhenzhen Du[1] · Ghulam Muhae-Ud-Din[1] · Dandan Qin[1] · Taiguo Liu[1] · Wanquan Chen[1] · Li Gao[1]

Received: 7 April 2022 / Accepted: 17 January 2023 / Published online: 9 February 2023

Abstract

Tilletia controversa Kühn is the causal agent of dwarf bunt disease in wheat. Understanding the infection of *T. controversa* is of practical and scientific importance for disease management. Here, we used scanning electron microscopy to characterize the histological changes at the seedling (Z12) and stem elongation stages (Z31) in resistant and susceptible wheat cultivars after *T. controversa* infection. At the seedling stage (Z12), the structure of stem and mesophyll cells slightly deformed after pathogen infection, but this deformation was greater in the susceptible cultivar than in the resistant cultivar. At the stem elongation stage (Z31), the structures of root parenchyma and epidermal cells were deformed more than at the seedling stage (Z12) for both the resistant and susceptible cultivars.

Keywords *Tilletia controversa* Kühn · Seedling stage (Z12) · Stem elongation (Z31) · Roots · Stem · Mesophyll

Introduction

Wheat (*Triticum aestivum*) is one of the most important staple food crops. China produces over 120 million tons of wheat per year. Wheat is the third most important crop overall, after rice and maize (Huang et al. 2015). Z12 and Z31 on the Zadoks scale provide the most complete description of wheat plant growth stages (Tottman et al. 1979). Disease, a main biotic stress, intensely affects plant productivity, growth, and reduces the quality and quantity of infected plants. Dwarf bunt, which infects wheat, is a soilborne disease caused by the fungus *Tilletia controversa*, which belongs to class Basidiomycetes and requires low temperature (5 °C) for spore germination (Muhae-Ud-Din, et al. 2020a, b; Liu et al. 2020). *T. controversa* is a quarantine pathogen and remains a major issue for trade between the People's Republic of China (PRC) and the United States of America (USA) (Mathre 1996). Yield losses can reach up to 70–80% under severe infection in cold areas (Purdy et al. 1963). *T. controversa* infection can cause alterations in the cellular and subcellular structures of susceptible plants more severely than resistant plants (Ren et al. 2021). The root epidermal, leaf mesophyll, and vascular tissues are more severely infected in susceptible cultivar than in resistant cultivar at the tillering stage (Z21) after *T. controversa* infection (Xu et al. 2021).

Epidermal cells have key roles in plant defence to protect cellular organelles (Lindenthal et al. 2005; Berger et al. 2007; Nadal and Flexas 2018; Xu et al. 2021). Mesophyll cells have an important role in photosynthesis and provide energy to plants (Vallad and Subbarao 2008). CO_2 diffusion through mesophyll cells is a complex process that determines the rate of photosynthesis in plants (Nadal and Flexas 2018). Plant pathogens alter the normal structures of epidermal and mesophyll cells (Lindenthal et al. 2005; Berger et al. 2007), but tissue alterations are more common in susceptible cultivars than in resistant cultivars (Muhae-Ud-Din et al. 2020a, b; Xu et al. 2021). The epidermal and mesophyll cells of susceptible cultivars were more infected than those of resistant cultivars of lettuce crops after *Verticillium dahlia* infection (Vallad and Subbarao 2008). Pereira et al. observed differences in the infection process of *Fusarium oxysporum* f. sp. *phaseoli* in bean cultivars and found that xylem cells of the resistant cultivar produced blocking substances that prevent the spread of fungi (Pereira et al. 2013). Fungal hyphae

Mekuria Wolde and Zhenzhen Du contributed equally to this work.

✉ Li Gao
xiaogaosx@hotmail.com

[1] State Key Laboratory for Biology of Plant Disease and Insect Pests, Institute of Plant Protection, Chinese Academy of Agricultural Sciences, Beijing 100193, China

in wheat-resistant cultivars were generally retarded compared with the spread and development of hyphae in tissues of susceptible cultivars (Hansen 1958; Xu et al. 2021). The epidermal and mesophyll cells of resistant cultivars were infected slightly compared with susceptible wheat cultivars (Woolman 1930). *Rhynchosporium secalis* alters the plasma membrane structure and cytoplasmic materials in susceptible cultivars of barley, but colonization of hyphae was retarded in the cell wall of resistant cultivars (Xi et al. 2000). *F. oxysporum* and *F. solani* infect xylem vessels and mitochondria only in susceptible cultivars of purple passion fruit (Ortiz et al. 2014). In grapes, callose and secretions were deposited around the stomata in the resistant cultivar, whereas neither callose nor secretion was observed in the susceptible cultivar (Gindro et al. 2003). Similarly, *Sclerotinia sclerotiorum* growth was impeded at 24 hpi only in resistant rapeseed (Garg et al. 2013). *Puccinia striiformis* f. sp. *tritici* only infects susceptible cultivars and changes plant morphology (Moldenhauer et al. 2006). Until now, important plant growth stages (seedling growth and stem elongation) in wheat against *T. controversa* were not investigated. We describe here the histopathological changes at seedling growth (Z12) and stem elongation (Z31) in roots, stems, and leaves in resistant and susceptible wheat cultivars in response to *T. controversa*.

Materials and methods

Plant and fungal materials

Wheat (*Triticum aestivum* L.) cv. Mianyang 26 and CU42 seeds were collected from the Institute of Plant Protection, Chinese Academy of Agricultural Sciences, China. Mianyang 26 is resistant, and CU42 is susceptible to *T. controversa*. Blair Goates kindly provided the pathogenic fungus *T. controversa* from the United States Department of Agricultural, Agricultural Research Service (USDA, ARS), Idaho, USA.

Culture of *T. controversa* teliospores

The adjusted concentration (approximately 100×10^6) of *T. controversa* teliospores was cultured on 2% soil agar medium plates. The cultured plates were placed in an incubator (MLR-352H, Japan) at 5 °C and 50% relative humidity for 60 days. Teliospore germination and hyphal growth were observed under a fully automatic inverted research grade microscope (IX83, OLYMPUS, Japan). Fungal mycelium was harvested in laminar flow using 5 mL ddH_2O (TransGen, China) in laminar flow maintaining a 10^6 cfu/mL concentration and the suspension was stored at 5 °C in an incubator (MLR-352H, Japan) until injection into the plants.

Inoculation of *T. controversa* in plants

Wheat plants were grown in pots under a 14 h light/10 h dark (5 ± 2 °C and 70% RH) regime. The pots were filled with soil and organic matter at a ratio of 2:1 and kept in a growth chamber (ARC-36, Percival, USA). Ten plants were planted in every pot of both cultivars. Fifty plants were inoculated with *T. controversa* hyphae at the seedling growth stage (Z11) by following the method of our laboratory (Muhae-Ud-Din et al. 2020a, b), and fifty plants were used as controls of both cultivars. The inoculation was repeated after a 1-day interval, and the fungal hyphal injections continued for 5 days. After successful infection, thirty plants of both resistant and susceptible cultivars were selected for scanning electron microscopy. The same number of plants was selected from the control group for microscopy. Plants treated with ddH_2O (TransGen, China) were used as the control group in this study.

Molecular detection of *T. controversa*

DNA was extracted from wheat leaves using a DNA extraction kit (Tiangen, China) by following the kit instructions. The DNA concentration was adjusted to 1 µg/µL for each sample. The sequence characterized amplified region (SCAR) marker was used for molecular detection of the pathogen. The primer sequences for the SCAR marker were ISSR859-140AF: 5′-TGGTGGTCG GGAAAGATTAGA-3 and ISSR859-511AR: 5′-GGG ACGAAGGCATCAAGAAG-3′. The PCR amplification procedure was as follows: initial denaturation at 94 °C for 5 min, followed by 30 cycles of amplification with denaturation at 94 °C for 20 s, annealing at 94 °C for 30 s, and extension at 72 °C for 30 s, and then a final extension at 72 °C for 7 min. After PCR, gel electrophoresis was performed at 150 V for 30 min, gel was stained with ethidium bromide (APE × BIO), and expected bands were visualized using the gel documentation system (WSE-5200 Printgraph 2 M, ATTO, Korea). Successful infection was indicated by positive amplification of 372 bp.

Scanning electron microscopy

The roots, leaves, and stems of fungi-infected and control plants at the Z12 and Z31 stages were collected from both cultivars and washed with ddH_2O for further

processing. Twenty five plants were used for Z12 stage, while remaining twenty five plants were used for Z31 stage for fungi-infected and control plants. The root and stem segments adjacent to the base were taken and sectioned to lengths of 5 mm, whereas leaf segments were adjusted to 5 mm × 5 mm in length and width, respectively. Samples were immediately placed in a 3% glutaraldehyde solution for solidification for 48 h and then washed with phosphoric acid buffer (APE × BIO) several times to remove the excess glutaraldehyde; they were stored in osmium acid (OSO4) (1%) (APE × BIO) at room temperature (25 °C) for 1.5 h. Subsequently, dehydration was carried out in a series of ethanol (APE × BIO) concentrations (30%, 50%, 60%, 70%, 80%, 90%, 95%, and 100%), and the dehydration time of each stage was more than 20 min. After dehydration with an ethanol gradient and osmium acid (APE × BIO), the critical carbon dioxide (CO_2) point drying method was used to dry the sample (Segado et al. 2016). The samples were sprayed with a gold metal film and observed under a scanning electron microscope (S-570, HITACHI, Japan) (Segado et al. 2016).

Results

Molecular detection of *T. controversa*

Successful infection was confirmed by specific amplification (372 bp) of *T. controversa* DNA in both resistant and susceptible cultivars (Fig. S1). After conformation, samples were subjected to scanning electron microscopy (SEM) investigation.

Comparison of root, stem, and leaf tissue structures of resistant and susceptible cultivars using scanning electron microscopy at the seedling growth stage (Z12)

Based on the resistant and susceptible cultivars, in root cells, as shown in Fig. 1, there were large differences in the parenchyma cells of fungi-infected plants of the susceptible cultivar compared with their control plants. The size of the xylem tissues in parenchyma cells of infected samples was large and loose compared with control samples (Fig. 1a, b); however, few differences were observed in parenchyma cells of infected and control samples of the resistant cultivar (Fig. 1e, f). Histological changes were observed in root epidermal cells of fungi-infected and control samples in both cultivars. In the infected susceptible cultivar, epidermal cells were severely infected, loosely arranged, and fungal damage was observed on the epidermal cells (Fig. 1d), but in control samples, the epidermal cells were compact, dense, and closely packed (Fig. 1c). However, there was no obvious change in epidermal cells of the resistant cultivar in either fungal-infected or control samples (Fig. 1g, h). Additionally, there is no obvious difference in parenchyma cells (Fig. 1a, e) and epidermal cells (Fig. 1c, g) of control resistant and susceptible plants. However, some structural differences were noted, which might be of genotype difference of both cultivars.

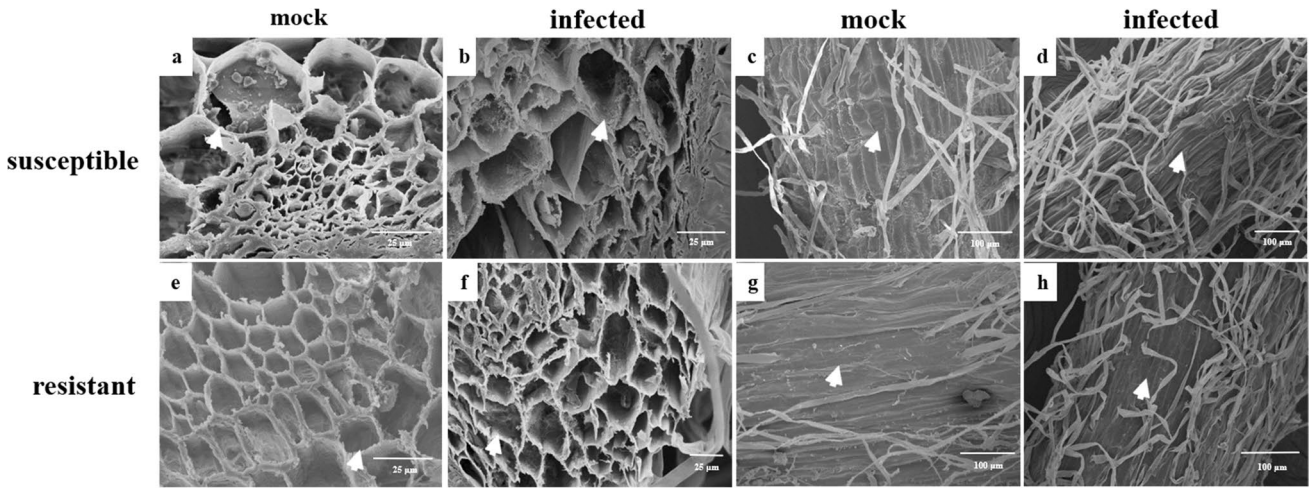

Fig. 1 Histological characteristics of root tissues at the seedling growth stage (Z12). **a** Parenchyma cells of the control plants in the susceptible cultivar, **b** parenchyma cells of the infected plants in the susceptible cultivar, **c** epidermal cells of the control plants in the susceptible cultivar, **d** epidermal cells of the infected plants in the susceptible cultivar, **e** parenchyma cells of the control plants in the resistant cultivar, **f** parenchyma cells of the infected plants in the resistant cultivar, **g** epidermal cells of the control plants in the resistant cultivar, and **h** epidermal cells of the infected plants in the resistant cultivar. White arrows in **a**–**h** indicate parenchyma cells and epidermal cells of roots. Scale bars, abef = 25 µm and cdgh = 100 µm

For the stem cells, plants of the first node were examined by scanning electron microscopy. The stem vascular system of the fungus-infected susceptible cultivar was loose and reduced in rigidity, and most stem cells changed their shape compared with those in the control susceptible cultivar (Fig. 2a, b). However, the stem vascular system of the fungus-infected resistant cultivar and their control samples did not share any obvious symptoms (Fig. 2c, d).

For the mesophyll cells, fungi-infected leaves and their respective controls of both resistant and susceptible cultivars were examined under scanning electron microscopy. The results revealed that few differences were observed in the samples of the infected susceptible cultivar and their respective controls; vascular bundles were closely packed in the control group compared with the infected group (Fig. 3a, b). However, no obvious differences were noted between the fungus-infected resistant cultivar and the control group (Fig. 3c, d). All the above results indicated that fungal hyphae affected root, stem, and leaf tissues of the susceptible cultivar more harshly than those of the resistant cultivar at the Z12 stage.

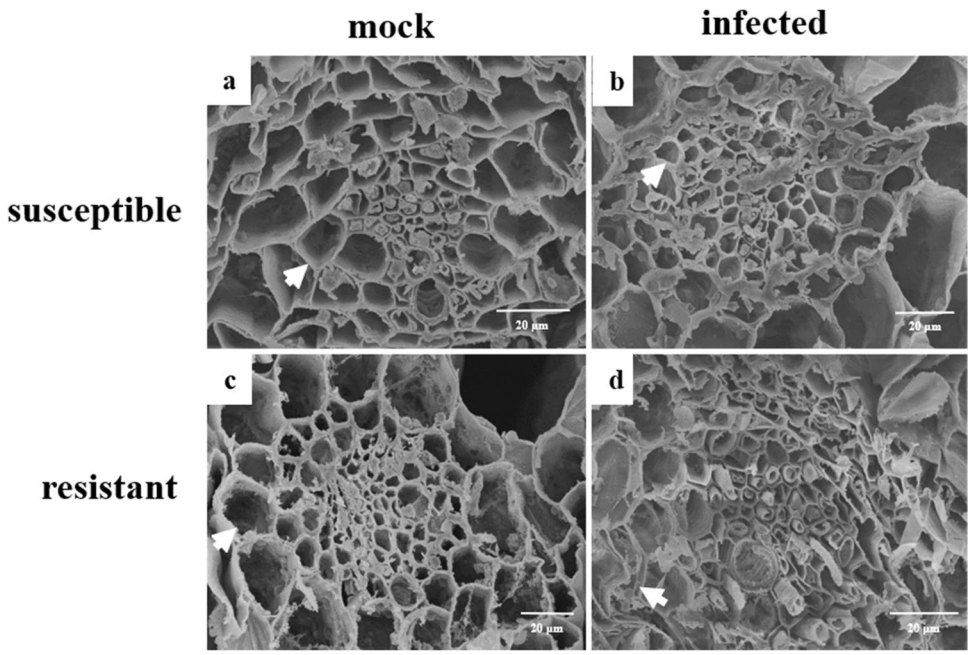

Fig. 2 Histological characteristics of stem tissues at the seedling growth stage (Z12). **a** Stem cell structure of the control plants in the susceptible cultivar, **b** stem cell structure of the infected plants in the susceptible cultivar, **c** stem cell structure of the control plants in the resistant cultivar, and **d** stem cell structure of the infected plants in the resistant cultivar. White arrows in **a**–**d** indicate vascular bundles in stem cells. Scale bar = 20 µm

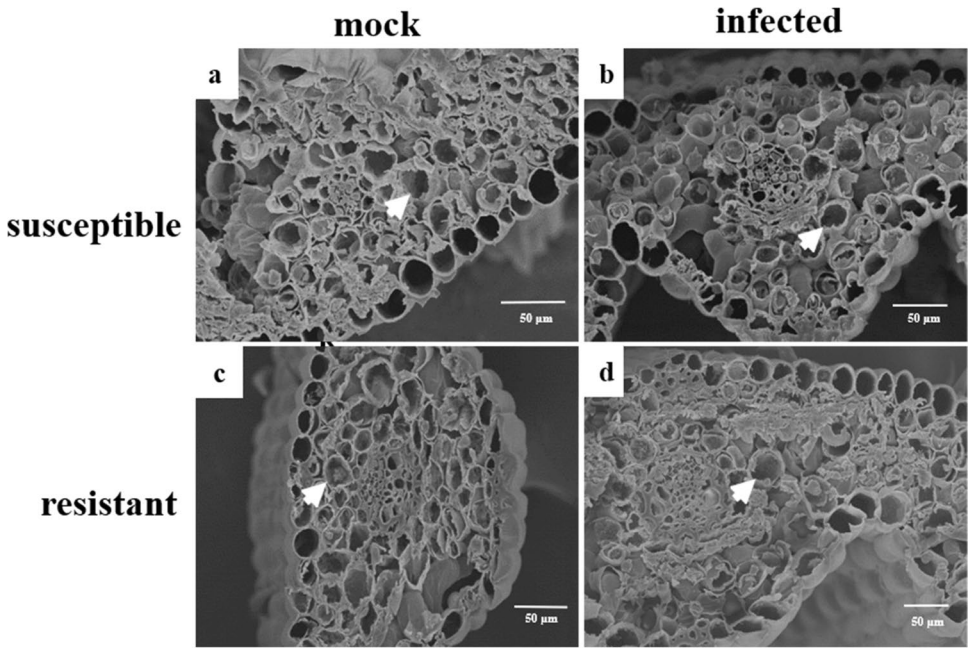

Fig. 3 Histological characteristics of leaf tissues at the seedling growth stage (Z12). **a** Mesophyll cells of the control plants in the susceptible cultivar, **b** mesophyll cells of the infected plants in the susceptible cultivar, **c** mesophyll cells of the control plants in the resistant cultivar, and **d** mesophyll cells of the infected plants in the resistant cultivars. White arrows in **a**–**d** indicate mesophyll cells in leaves. Scale bar = 50 µm

Comparison of root, stem, and leaf tissue structures of resistant and susceptible cultivars using scanning electron microscopy at the stem elongation stage (Z31)

The roots, stems, and leaves of fungi-infected resistant and susceptible cultivars and their respective controls were also examined at the stem elongation stage (Z31) for further confirmation. At the stem elongation stage (Z31), parenchyma cells of resistant and susceptible roots were examined under scanning electron microscopy. The parenchyma cells of the susceptible cultivar were damaged, and fungal hyphae were seen in the vascular tissues of parenchyma cells compared with control samples (Fig. 4a, b). For parenchyma cells, the morphology of the resistant cultivar did not show any obvious changes between fungi-infected and control samples (Fig. 4e, f). For epidermal cells of roots for Z31, root epidermal cells of the fungal infected susceptible cultivar were harshly damaged, vascular bundles lost their strength, root hairs were sparse, and fungal hyphae were seen on epidermal cells (Fig. 4d). In the control group, the epidermal cells were closely packed (Fig. 4c). We found fungal hyphae in root epidermal cells of the fungus-infected resistant cultivar, and slight damage was observed in cells compared with control samples (Fig. 4g, h).

For the stem cells, fungi-infected, control resistant, and susceptible cultivars were analyzed at the Z31 stage. As shown in Fig. 5, the vascular system of the stem of the fungus-infected susceptible cultivar was harshly infected, vascular pores were filled with hyphae, and the shape of the cells changed compared with that of the control group (Fig. 5a, b). In contrast, the stem vascular system between fungi-infected resistant and fungi-susceptible cultivars was not obviously infected and showed a similar vascular system structure (Fig. 5c, d).

For leaf mesophyll cells at Z31, the infected susceptible cultivar showed cell abnormalities, including vascular bundles that were loosely packed and pores in vascular bundles that increased in size (Fig. 6b). However, in the control samples, the mesophyll cells were normal (Fig. 6a). In the resistant cultivar, very slight modifications were observed in mesophyll cells of fungus-infected samples (Fig. 6d) compared with control samples (Fig. 6c). All of the above results showed that *T. controversa* infected and changed the morphology of roots, stems, and leaves more harshly in the susceptible cultivar than in the resistant cultivar at seedling growth (Z12) and stem elongation (Z31).

Discussion

In this study, scanning electron microscopy was used to investigate the histological changes in resistant and susceptible cultivars at the Z12 and stem Z31 stages against *T. controversa*, which showed compatibility between *T. controversa* and wheat plants. In the susceptible cultivar, fungal hyphae reached the growing point most early by following the spaces of connective cells and deformed the parenchyma and epidermis cells in both the Z12 and Z31 stages. From these infected sites, mycelia became

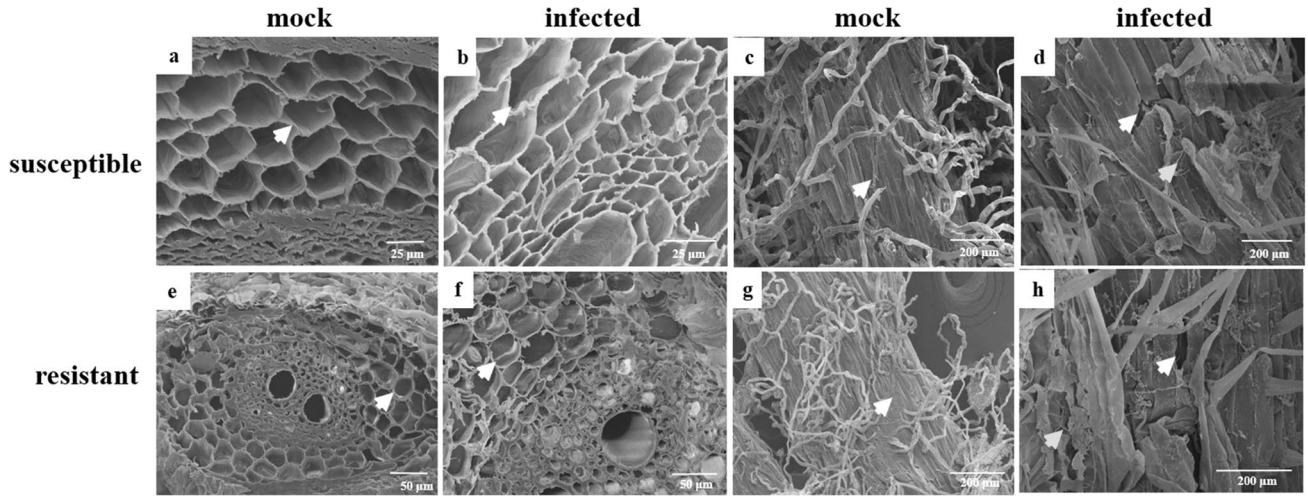

Fig. 4 Histological characteristics of the root tissues at the elongation stage (Z31). **a** Parenchyma cells of the control susceptible cultivar, **b** parenchyma cells of the infected plants in the susceptible cultivar, **c** epidermal cells of the control plants in the susceptible cultivar, **d** epidermal cells of the infected plants in the susceptible cultivar, **e** parenchyma cells of the control plants in the resistant cultivar, **f** parenchyma cells of the infected plants in the resistant cultivar, **g** epidermal cells of the control plants in the resistant cultivar, and **h** epidermal cells of the infected plants in the resistant cultivar. White arrows in **a**–**h** indicate parenchyma cells and epidermal cells of roots. Yellow arrows in **d**, **h** indicate hyphae in the epidermal cells. Scale bars, ab = 25 μm, ef = 50 μm, and cdgh = 200 μm

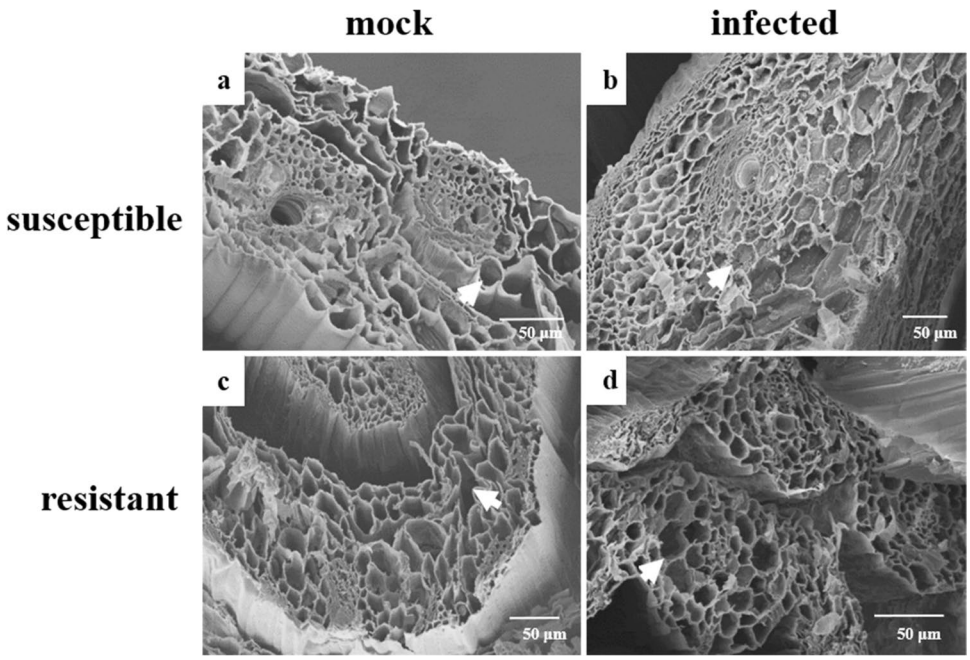

Fig. 5 Histological characteristics of stem tissues at the stem elongation stage (Z31). **a** Stem cell structure of the control plants in the susceptible cultivar, **b** stem cell structure of the infected plants in the susceptible cultivar, **c** stem cell structure of the control plants in the resistant cultivar, and **d** stem cell structure of the infected plants in the resistant cultivar. White arrows **a**–**d** indicate vascular bundles in stem cells. Scale bar = 50 µm

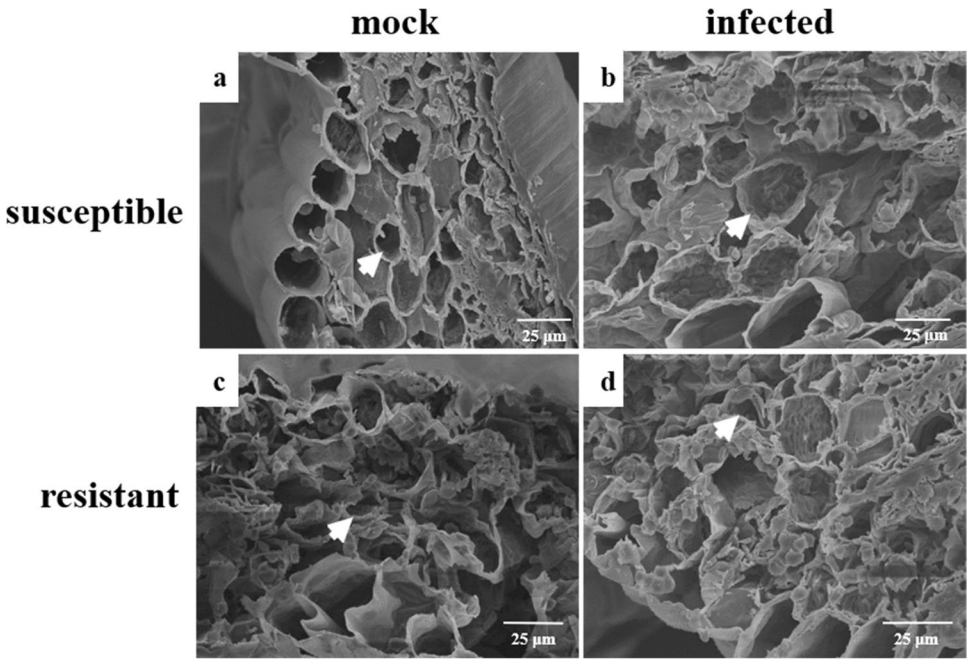

Fig. 6 Histological characteristics of leaf tissues at the stem elongation stage (Z31): **a** mesophyll cells of the control plants in the susceptible cultivar, **b** mesophyll cells of the infected plants in the susceptible cultivar, **c** mesophyll cells of the control plants in the resistant cultivar, and **d** mesophyll cells of the infected plants in the resistant cultivar. White arrows in **a**–**d** indicate mesophyll cells in leaves. Scale bar = 50 µm

permanently established at the growing point, and tillers initiated, always before intermodal elongation, and thus assured sporulation of the fungus. According to the results, the parenchyma cells, epidermal cells, and mesophyll cells of the susceptible cultivar were much more affected by *T. controversa* at Z12 and Z31 than those of the resistant cultivar. Our interpretation of fungal development of *T. controversa* in the susceptible cultivar is similar to that described by Xu et al. (2021) in their studies. Other reports showed that the growth of *P. striiformis* was retarded in wheat-resistant cultivars compared with susceptible cultivars (Zhang et al. 2012; Riaz and Hickey 2019). Structural alterations were seen in the tissues of only resistant cultivars after pathogen infection, including the formation of elicitor substances in xylem cells (Shi et al. 1992; Hall et al. 2011), callose (Gindro et al. 2003), reactive oxygen species (Lu and Yao 2018), tyloses (Bishop and Cooper 1984; Zhang et al. 2015), and

the formation of gel proteins (Andersen et al. 2018). The parenchyma cells of resistant plants were more compact, similar to that described by Pereira et al. (2013) in their studies. The vascular bundles were more compact and closely packed in resistant cultivars than in susceptible cultivars (Hall et al. 2011). Some studies have shown that epidermal cells of resistant plants alter after pathogen infection for some time and then recover to a normal shape (Xi et al. 2000). The formation of a protective layer of lignin, cellulose, and arabinoxylan molecules in the cell wall of resistant plants in response to *Sporisorium scitamineum* infection can increase the resistance level against pathogens (Marques et al. 2018). Nutrient uptake from the vascular bundle of stem cells easily occurred in resistant plants compared with susceptible plants after *Rhynchosporium secalis* infection (Xi et al. 2000). Based on our findings, we agree with Fernandez and Ruben Duran (1978) and Xu et al. (2021) that hyphae affect and alter the morphological structures much more harshly in wheat-susceptible cultivars than in wheat-susceptible cultivars. Leaf mesophyll cells are key players in the photosynthetic process and have a role in increasing resistance against pathogens (Scholes and Rolfe 2004; Ren et al. 2021). Our results showed that mesophyll cells of the susceptible cultivar were dramatically affected by *T. controversa* at both the Z12 and Z31 stages but not in the resistant cultivar. Our root cell results support the results of Zhang et al. (2015), in which *Fusarium oxysporum* f. sp. *niveum* dramatically altered the structures of root cells in the susceptible cultivar compared with the resistant cultivar. All of the above results indicated that *T. controversa* affects the roots, stems, and leaf cells of the susceptible cultivar much more severely than those of the resistant cultivar at both the Z12 and Z31 stages. In conclusion, *T. controversa* penetrates root tissues during the seedling stage and then proliferates to the above parts of the plants. With the increase in hyphae in later periods, alterations in the tissues and cells increased, including stem and leaf tissues, which will provide important information on the response of wheat to the pathogen.

Supplementary Information The online version contains supplementary material available at https://doi.org/10.1007/s40858-023-00555-y.

Author contribution L. G. designed the experiment and wrote the manuscript; M. W. performed the experiment; G. M., D. Z., and D. Q. revised the manuscript; and W. C. and T. L. provided the materials. All authors were involved in writing the paper and gave final approval to publish the manuscript.

Funding This work was supported by the National Natural Science Foundation of China (31761143011).

Data availability The datasets generated during and/or analyzed during the current study are available from the corresponding author on reasonable request.

Declarations

Conflict of interest The authors declare no competing interests.

References

Scholes JD, Rolfe SA (2004) Chlorophyll fluorescence imaging as tool for understanding the impact of fungal diseases on plant performance: a phenomics perspective. Functional Plant Biology 36:880–892

Andersen EJ, Ali S, Byamukama E, Yen Y, Nepal MP (2018) Disease resistance mechanisms in plants. Genes 9:339

Berger S, Sinha AK, Roitsch T (2007) Plant physiology meets phytopathology: plant primary metabolism and plant-pathogen interactions. Journal of Experimental Botany 58:4019–4026

Bishop CD, Cooper RM (1984) Ultrastructure of vascular colonization by fungal wilt pathogens. II. Invasion of resistant cultivars. Physiological Plant Pathology 24:277–289

Fernandez JH, Ruben Duran SJ (1978) Histological aspects of dwarf bunt resistance in wheat. Phytopathology 68:1417–1421

Garg H, Li H, Sivasithamparam K, Barbetti MJ (2013) Differentially expressed proteins and associated histological and disease progression changes in cotyledon tissue of a resistant and susceptible genotype of *Brassica napus* infected with *Sclerotinia sclerotiorum*. PLoS One 8:e65205

Gindro K, Pezet R, Viret O (2003) Histological study of the responses of two Vitis vinifera cultivars (resistant and susceptible) to *Plasmopara viticola* infections. Plant Physiology and Biochemistry 41:846–853

Hall C, Heath R, Guest DI (2011) Rapid and intense accumulation of terpenoid phytoalexins in infected xylem tissues of cotton (*Gossypium hirsutum*) resistant to *Fusarium oxysporum f.sp. vasinfectum*. Physiological and Molecular Plant Pathology 76:182–188

Hansen F (1958) Anatomische untersuchungen uber eindringen and ausbreitung von Tilletia-Arten in getreidepflanzen in abhangigkeit vom entwichlungszustand der wirtspflanze. Phytopathology 34:169–208

Riaz A, Hickey LT (2019) Rapid phenotyping adult plant resistance to stem rust in wheat grown under controlled conditions. In wheat rust diseases. Humana Press, New York, pp 183–196

Huang J, Xiang C, Wang Y (2015) The impact of CIMMYT wheat germplasm on wheat productivity in China. CIMMYT, CGIAR, pp 1–21

Lindenthal M, Steiner U, Dehne HW, Oerke EC (2005) Effect of downy mildew development on transpiration of cucumber leaves visualized by digital infrared thermography. Phytopathology 95:233–240

Liu J, Li C, Muhae-Ud-Din G, Liu T, Chen W, Zhang J, Gao L (2020) Development of the droplet digital PCR to detect the teliospores of *Tilletia controversa* Kühn in the soil with greatly enhanced sensitivity. Frontiers in Microbiology 11:4

Lu Y, Yao J (2018) Chloroplasts at the crossroad of photosynthesis, pathogen infection and plant defense. International Journal of Molecular Sciences 19:3900

Marques JP, Hoy JW, Appezzato-da-Glória B, Viveros AF, Vieira ML, Baisakh N (2018) Sugarcane cell wallassociated defense responses to infection by *Sporisorium scitamineum*. Frontiers in Plant Science 9:698

Mathre DE (1996) Dwarf bunt: politics, identification, and biology. Annual Review of Phytopathololgy 34:67–85

Moldenhauer J, Moerschbacher BM, Van Der Westhuizen AJ (2006) Histological investigation of stripe rust (*Puccinia striiformis* f.sp. *tritici*) development in resistant and susceptible wheat cultivars. Plant Pathology 55:469–474

Muhae-Ud-Din G, Chen D, Liu T, Chen W, Gao L (2020) Characterization of the wheat cultivars against *Tilletia controversa* Kühn, causal agent of wheat dwarf bunt. Scientific Reports 10:9029

Muhae-Ud-Din G, Chen D, Liu T, Chen W, Gao L (2020) Methyljasmonate and salicylic acid contribute to the control of *Tilletia controversa* Kühn, causal agent of wheat dwarf bunt. Scientific Reports 10:19175

Nadal M, Flexas J (2018) Mesophyll conductance to CO2 diffusion: effects of drought and opportunities for improvement. In Water scarcity and sustainable agriculture in semiarid environment. Academic Press, pp 403–438

Ortiz E, Cruz M, Melgarejo LM, Marquínez X, Hoyos-Carvajal L (2014) Histopathological features of infections caused by *Fusarium oxysporum* and *F. solani* in purple passion fruit plants (Passiflora edulis Sims). Summa Phytopathology 40:134–140

Pereira AC, Cruz MFA, Paula Júnior TJ, Rodrigues FA, Carneiro JES, Vieira RF, Carneiro PCS (2013) Infection process of *Fusarium oxysporum f. sp. phaseoli* on resistant, intermediate and susceptible bean cultivars. Tropical Plant Pathology 38:323–328

Purdy LH, Meiners JP, Hoffmann JA, Stewart VR (1963) Time of year of infection of winter wheat by dwarf bunt fungus. Phytopathology 53:1419

Ren Z, Zhang W, Wang M, Gao H, Shen H, Wang C, Gao L (2021) Characteristics of the infection of *Tilletia laevis* Kühn (syn. *Tilletia foetida* (Wallr.) Liro.) in compatible wheat. Plant Pathology Journal 37:447–445

Segado P, Domínguez E, Heredia A (2016) Ultrastructure of the epidermal cell wall and cuticle of tomato fruit (*Solanum lycopersicum* L.) during development. Plant Physiology 170:935–946

Shi J, Mueller WC, Beckman CH (1992) Vessel occlusion and secretory activities of vessel contact cells in resistant or susceptible cotton plants infected with *Fusarium oxysporum f.sp. vasinfectum*. Physiological and Molecular Plant Pathology 40:133–147

Tottman DR, Makepeace RJ, Broad H (1979) An explanation of the decimal code for the growth stages of cereals, with illustrations. Annals of Applied Biology 93:221–234

Vallad GE, Subbarao KV (2008) Colonization of resistant and susceptible lettuce cultivars by a green fluorescent protein-tagged isolate of *Verticillium dahliae*. Phytopathology 98:871–885

Woolman H (1930) Infection phenomena and host reactions caused by *Tilletia tritici* in susceptible and non-susceptible varieties of wheat. Phytopathology 20:637–652

Carisse KX, Burnett PA, Tewari JP, Chen MH, Turkington TK, Helm JH (2000) Histopathological study of barley cultivars resistant and susceptible to *Rhynchosporium secalis*. Phytopathology 90:94–102

Xu T, Qin D, Din Muhae Ud, G, Liu T, Chen W, Gao L, (2021) Characterization of histological changes at the tillering stage (Z21) in resistant and susceptible wheat plants infected by *Tilletia controversa* Kühn. BMC Plant Biology 21:49

Zhang H, Wang C, Cheng Y, Chen X, Han Q, Huang L, Kang Z (2012) Histological and cytological characterization of adult plant resistance to wheat stripe rust. Plant cell reports 31:2121–2137

Zhang M, Xu JH, Liu G, Yao XF, Li PF, Yang XP (2015) Characterization of the watermelon seedling infection process by Fusarium oxysporum f. sp. niveum. Plant Pathology 64:1076–1084